

**Integrated Model of Chemical Perturbations of a Biological Pathway
Using 18 In Vitro High Throughput Screening Assays for the Estrogen Receptor**

Journal:	<i>Toxicological Sciences</i>
Manuscript ID:	TOXSCI-15-0258.R1
Manuscript Type:	Research Article
Date Submitted by the Author:	n/a
Complete List of Authors:	Judson, Richard S.; US EPA, National Center for Computational Toxicology Magpantay, Felicia Maria; University of Michigan, Department of Mathematics Chickarmane, Vijay; California Institute of Technology, Division of Biology Haskell, Cymra; University of Southern California, Department of Mathematics Tania, Nussy; Smith College, Department of Mathematics Taylor, Jean; New York University, Courant Institute Xia, Menghang; National Center for Advancing Translational Sciences, National Institutes of Health, NIH Chemical Genomics Center Huang, Ruili; NIH, NIH Chemical Genomics Center Rotroff, Daniel M.; North Carolina State University, Bioinformatics Research Center Filer, Dayne L.; US EPA, ORISE Fellow at the U.S. EPA Houck, Keith; USEPA, NCCT Martin, Matthew; US EPA, Sipes, Nisha; NIH, National Toxicology Program Richard, Ann; USEPA, MD B143-06 Mansouri, Kamel; US EPA, ORISE Fellow at the U.S. EPA Setzer, R.; USEPA, Mail Drop B143-05 Knudsen, Thomas; US EPA, NCCT Crofton, Kevin; USEPA, Neurotoxicology Division (MD-74B) Thomas, Russell S.; EPA,
Key Words:	biological modeling < Risk Assessment, endocrine disruptors < Endocrine Toxicology, endocrine; estrogens < Endocrine Toxicology, receptor; nuclear hormone < Gene Expression/Regulation, alternatives to animal testing < In Vitro and Alternatives, bioinformatics < Methods
Society of Toxicology Specialty Section Subject Area:	Biological Modeling [103]



1
2
3
4
5
6
7
8
9
10
11
12
13
14
15
16
17
18
19
20
21
22
23
24
25
26
27
28
29
30
31
32
33
34
35
36
37
38
39
40
41
42
43
44
45
46
47
48
49
50
51
52
53
54
55
56
57
58
59
60

**Integrated Model of Chemical Perturbations of a Biological Pathway
Using 18 *In Vitro* High Throughput Screening Assays for the Estrogen Receptor**

Richard S. Judson(1), Felicia Maria Magpantay(2), Vijay Chickarmane(3), Cymra Haskell(4), Nessy Tania(5), Jean Taylor(6), Menghang Xia(7), Ruili Huang(7), Daniel M. Rotroff(8,9), Dayne L. Filer(10), Keith A. Houck(1), Matthew T. Martin(1), Nisha Sipes(11), Ann M. Richard(1), Kamel Mansouri(10), R. Woodrow Setzer(1), Thomas B. Knudsen(1), Kevin M. Crofton(1), Russell S. Thomas(1)

(1) U.S. Environmental Protection Agency, Research Triangle Park NC, 27711 USA

(2) Department of Mathematics, University of Michigan, Ann Arbor MI, 48109 USA

(3) Division of Biology, California Institute of Technology, Pasadena CA, 91125 USA

(4) Department of Mathematics, University of Southern California, Los Angeles CA, 90089 USA

(5) Department of Mathematics, Smith College, Northampton MA, 01063 USA

(6) Courant Institute, New York University, New York NY, 10012 USA

(7) NIH Chemical Genomics Center, National Center for Advancing Translational Sciences, Rockville MD, 20892 USA

(8) North Carolina State University, Department of Statistics, North Carolina State University, Raleigh, NC, 27607 USA

(9) Bioinformatics Research Center, North Carolina State University, Raleigh, NC, 27607 USA

(10) ORISE Fellow at the U.S. EPA, Research Triangle Park NC, 27711 USA

11) NIH National Toxicology Program, RTP NC 27711 USA

RJ: judson.richard@epa.gov

FMM: felicigm@umich.edu

VC: vchickar@caltech.edu

CH: chaskell@usc.edu

NT: ntania@smith.edu

JT: jtaylor@cims.nyu.edu

DR: daniel.rotroff@ncsu.edu

DF: filer.dayne@epa.gov

KH: houck.keith@epa.gov

MM: martin.matt@epa.gov

NS: nisha.sipes@nih.gov

AR: richard.ann@epa.gov

TH: knudsen.thomas@epa.gov

MX: mxia@mail.nih.gov

RH: huangru@mail.nih.gov

1
2
3
4
5
6
7
8
9
10
11
12
13
14
15
16
17
18
19
20
21
22
23
24
25
26
27
28
29
30
31
32
33
34
35
36
37
38
39
40
41
42
43
44
45
46
47
48
49
50
51
52
53
54
55
56
57
58
59
60

KM: Mansouri.kamel@epa.gov
RWS: setzer.woodrow@epa.gov
KMC: crofton.kevin@epa.gov
RST: Thomas.russell@epa.gov

Abstract

We demonstrate a computational network model that integrates 18 *in vitro*, high-throughput screening assays measuring estrogen receptor (ER) binding, dimerization, chromatin binding, transcriptional activation and ER-dependent cell proliferation. The network model uses activity patterns across the *in vitro* assays to predict whether a chemical is an ER agonist or antagonist, or is otherwise influencing the assays through a manner dependent on the physics and chemistry of the technology platform (“assay interference”). The method is applied to a library of 1812 commercial and environmental chemicals, including 45 ER positive and negative reference chemicals. Among the reference chemicals, the network model correctly identified the agonists and antagonists with the exception of very weak compounds whose activity was outside the concentration range tested. The model agonist score also correlated with the expected potency class of the active reference chemicals. Of the 1812 chemicals evaluated, 111 (6.1%) were predicted to be strongly ER active in agonist or antagonist mode. This dataset and model were also used to begin a systematic investigation of assay interference. The most prominent cause of false-positive activity (activity in an assay that is likely not due to interaction of the chemical with ER) is cytotoxicity. The model provides the ability to prioritize a large set of important environmental chemicals with human exposure potential for additional *in vivo* endocrine testing. Finally, this model is generalizable to any molecular pathway for which there are multiple upstream and downstream assays available. *Disclaimer: The views expressed in this paper are those of the authors and do not necessarily reflect the views or policies of the U.S. Environmental Protection Agency.*

Keywords:

Estrogen receptor

EDSP

High-throughput screening

In vitro

Prioritization

Biological modeling

Introduction

Signaling pathways and networks are key components of complex biological systems. Endocrine signaling that commences when hormones interact with their cognate receptors initiate post-receptor events and downstream cellular consequences that can be altered by xenobiotic chemicals, either as mimetics to the natural ligands or as modulators to the upstream and/or downstream events. These perturbations may be efficacious in medicinal therapies (e.g., pharmaceuticals) or deleterious (e.g., environmental toxicants or off-target interactions for pharmaceuticals).

In order to measure the effect of xenobiotics on signaling pathways, a variety of *in vitro* assays have been widely used in drug development and toxicity testing programs. These range from biochemical assays using purified protein to more complex cellular assays that can respond to chemical perturbations in various ways. Each of these assays is subject to false positive and false negative results, some of which are the result of “assay interference”. Conceptually, assay interference (Auld, Thorne et al. 2008, Baell and Holloway 2010, Thorne, Auld et al. 2010, Bruns and Watson 2012) is a phenomenon whereby assays designed to measure binding to a protein or perturbation of a given pathway may produce false signals when the target protein itself, or other pathways in the system, are altered non-specifically. The standard approach to deal with assay interference issues is to deploy “orthogonal” assays (Miller, Thanabal et al. 2010, Thorne, Auld et al. 2010) that help distinguish activity towards the intended target or pathway from non-specific activities. In addition to assay interference issues, every assay has inherent limitations such as dynamic range or levels of background noise. Using a suite of assays to detect pathway perturbations may minimize potential non-specific effects or limitations of any single assay.

In this study, we evaluated ER pathway activity and assay interference using data from a collection of 18 *in vitro* assays that probe the estrogen receptor (ER) pathway in mammalian systems. These 18 *in vitro* assays are a subset of a larger collection of assays (821 individual assay endpoints) used in the EPA ToxCast program (Dix, Houck et al. 2007, Judson, Houck et al. 2010, Kavlock, Chandler et al. 2012). The 18 assays include biochemical and cell-based *in vitro* assays that probe perturbations of ER pathway responses at sites within the cell: receptor binding, receptor dimerization, chromatin binding of the mature transcription factor, gene transcription and changes in ER-induced cell growth kinetics (Figure 1). The battery of 18 *in vitro* assays was used to screen a library of 1812 chemicals. Included in the chemical library were reference chemicals, i.e., known ER agonists and antagonists, as well as a large number of commercial chemicals with reported estrogen-like activity, some of which are potentially selective estrogen receptor modulators (SERMs) (Dutertre and Smith 2000, Katzenellenbogen, Choi et al.

2000, Katzenellenbogen and Katzenellenbogen 2000, Katzenellenbogen, Montano et al. 2000, Diel, Oloff et al. 2001).

A subset of compounds would be expected to elicit activity in some, but perhaps not all assays, given the diversity of cell types and technologies included in the battery of 18 *in vitro* assays. To navigate this complexity, we developed a mathematical / statistical model to infer whether chemicals that activate specific patterns of the *in vitro* assays were more likely to be ER agonists, ER antagonists, or were more likely to be causing assay activity through specific types of assay interference. Previous modeling approaches have been developed using a subset of the data presented here (Reif, Martin et al. 2010, Rotroff, Martin et al. 2014), but the current approach provides a more generic model framework applicable to other signaling pathways beyond ER.

Understanding the results of this analysis will have three broad implications. First, the commercial chemicals identified as ER-pathway actives can be prioritized for further testing as endocrine disruptors. Because such testing is expensive and time consuming, there is value in reducing false positives without significantly increasing false negatives using these *in vitro* screens. Second, chemicals or chemical classes that show broad assay interference may potentially cause similar interference in other *in vitro* assays utilizing the same cell types or technology platforms. These chemicals can be flagged for extra scrutiny when analyzing results for other targets. Finally, methods developed here on this test case can be applied to the analysis of results for other assays and pathways beyond the ER responses.

Materials and Methods

Assays and Chemicals: The input data for the model includes chemical structures and concentration-response data for 18 ER-related *in vitro* assays, plus data for many non-ER *in vitro* assay endpoints (ranging from 186-821 assays, depending on the chemical). The data used were generated by the EPA ToxCast program (Dix, Houck et al. 2007, Judson, Houck et al. 2010). The dataset comprises concentration-response data on 1812 chemicals with full data on ER pathway *in vitro* assays. These include 3 cell-free biochemical radioligand ER binding assays [Novascreen / NVS: (Knudsen, Houck et al. 2011, Sipes, Martin et al. 2013)]; a set of 3 protein complementation assays that measure formation of ER dimers and test for activity against both ER-alpha and ER-beta, (each measured at 2 separate times for a total of 6 assay readouts) [Odyssey Thera / OT: (Filer 2015)]; 2 assays measuring interaction of the mature transcription factor with DNA [Odyssey Thera / OT: (Filer 2015)]; 2 transactivation assays measuring RNA transcript levels [Attagene / ATG: (Martin, Dix et al. 2010)]; 2 transactivation assays measuring reporter protein level readouts [Tox21: (Huang, Sakamuru et al. 2014)]; an ER-sensitive

cell proliferation assay [ACEA: (Rotroff, Dix et al. 2013)]; and 2 transactivation antagonist assays [Tox21: (Huang, Sakamuru et al. 2014)]. The assay sources refer to the company or laboratory where the assays were performed. The 18 *in vitro* assays used are summarized in Table 1 and more detail is given in Supplemental File S1, Appendix 1. The assay IDs correspond to Figure 1. The chemicals are listed in Supplemental File S2 along with summary results from subsequent analyses. The chemicals were run in concentration-response format in all *in vitro* assays except for the cell-free binding assays (NVS). The NVS assays were initially run at a single concentration (25 μ M), and if significant activity (3 median absolute deviation (MAD) above the median or 30% activity) was seen, the chemical was then run in concentration-response mode.

Reference chemicals: A set of 45 positive and negative reference chemicals were used to evaluate the performance of the model (described below). These chemicals have been used to validate ER *in vitro* assays and were taken from the OECD (Organisation for Economic Cooperation and Development) TG457 BG1 guidance document (OECD 2012). The reference chemicals and their expected potencies are listed in Supplemental File S1, Appendix 3.

Data Processing and Synthetic Concentration-Response Data: All of the concentration-response data were analyzed using a standardized data analysis pipeline, which automates the processes of baseline correction, normalization, curve-fitting, hit-calling and detection of a variety of potential confounders. This pipeline, along with all of the raw and processed data, and annotations is publicly available [<http://epa.gov/ncct/toxcast/data.html> and <http://actor.epa.gov/edsp21>]. All *in vitro* assays except the Attagene assays were normalized to the range 0-100%, using the response of 17 β -estradiol in the agonist group and 4-hydroxy-tamoxifen in the antagonist group. Attagene data were normalized as a fold-change over the solvent (DMSO) control and then multiplied by a factor of 25 to yield a range of approximately 0-100. The data from each chemical-assay pair is fit to three models: a constant model, a Hill model, and a Gain-Loss model. The latter allows the curve to rise from zero at low concentrations to a plateau, and then fall off again. This last curve shape allows us to account for non-specific assay interference, such as cytotoxicity occurring at high concentrations. To call an assay-chemical pair a “hit”, at least one concentration has to reach a significance threshold, operationally defined (typically) as 10 MAD around the baseline. The MAD is calculated per assay using the distribution of the lowest 2 concentration points for all chemicals run in the *in vitro* assay, around the median of those points whereby the assay baseline is set as the median. The Akaike Information Criterion (Akaike 1998) (AIC) is then calculated for each model, and the model with the lowest AIC is selected. For each model, the output includes parameters as well as a number of diagnostics. The diagnostics are assigned to specific chemical sample-assay pairs and indicate the

presence of potential confounding factors such as curves that are marginally active and could be the result of non-normally distributed background noise instead of true activity. An AC50 (activity concentration at half-maximal response), Hill-slope and maximum activity (T or Top value) are extracted. To allow computational synthesis across different *in vitro* assays with different experimental designs (i.e., different numbers of concentrations tested), a set of synthetic concentration-response activities was generated for each chemical-assay pair at standardized concentrations. This procedure used the experimentally derived AC50, Hill-slope and Top parameters and a Hill equation. All AC50 values were in μM , and the synthetic concentrations were a 1.5-fold dilutions series of 45 concentrations from 1 pM to 100 μM .

Accounting for cytotoxicity-related assay interference: For many chemicals, we observe that there are a large number of hits (positive assay responses) for ER and non-ER assays in the concentration range where cytotoxicity is observed. Cytotoxicity is measured using a collection of 35 assays in the ToxCast battery that detect cytotoxicity or other forms of cell loss across several cell lines and primary cell types. Because many non-selective cellular responses are invoked as the concentration tested reaches a critical point, we simply refer to this set of cytotoxicity-related hits as a “burst”. The following scheme is used to filter out these non-selective, cell-stress or cytotoxicity-related assay hits. For chemicals with two or more positive responses in cytotoxicity assays, we calculate the median $\log\text{AC50}(\text{cytotox})$ and the MAD of the $\log\text{AC50}(\text{cytotox})$ hits. Next, we calculate the median of the MAD of the $\log\text{AC50}(\text{cytotox})$ distributions across all chemicals to define the global cytotoxicity MAD. A new value (the Z-score) is then assigned to each *in vitro* assay hit:

$$Z(\text{chemical}, \text{assay}) = \frac{\log \text{AC50}(\text{chemical}, \text{assay}) - \text{median}[\log \text{AC50}(\text{chemical}, \text{cytotoxicity})]}{\text{MAD}_{\text{global}}} \quad (1)$$

If fewer than 2 cytotoxicity assays are hit, the median cytotoxicity concentration is arbitrarily set to 1000 μM , which simply sets all Z-values for assay hits to a value >3 . A hit with a large value of Z occurs at concentrations significantly below where cytotoxicity is occurring. This hit is more likely to be able to induce biological activity and/or toxicity through a target-selective mechanism. The global cytotoxicity MAD is 0.26 log units.

Structure of the Network Model: Figure 1 is a graphical representation of the network model used to evaluate the integrated *in vitro* assay responses. The model was based on the series of molecular events that typically occur in a nuclear receptor-mediated response (Mangelsdorf, Thummel et al. 1995, Gronemeyer, Gustafsson et al. 2004). The process starts with the interaction of a chemical with an ER (Receptor node R1). For

example, an ER agonist will cause the receptors to dimerize (node N1), translocate to the nucleus and recruit co-factors to form the complete active transcription factor complex (TF) (node N2). This TF binds to the chromatin DNA (node N3), initiates transcription of mRNA (node N4) and subsequent translation to protein (node N5). For ER agonist activity, one downstream consequence can be cell proliferation (node N6). Note that the temporal order of these process is not necessarily as depicted here. Each of these processes (with the exception of cofactor recruitment) was measured in the current collection of 18 *in vitro* assays (represented in the figure as white stars). Table 1 (see Methods) provides the assay ID (A1-A18) to match the associated *in vitro* assay on Figure 1 and a brief assay description. More detail is provided in Supplemental File S1 Appendix 1. The ER pathway is shown in two modes: agonist (blue) and antagonist (red). The model assumes that a chemical interacting with the ER will bind in one or both of the agonist or antagonist conformations and in turn, trigger activity in the appropriate pathway. Note that the model allows for the prediction of mixed agonist/antagonist activity.

In addition to ER-mediated effects, each individual *in vitro* assay is subject to processes that can lead to non-specific activity, independent of the ER pathway node that it is supposed to measure. The assay interference pathways were modeled as alternate “pseudo-receptors” (gray arrow nodes). The details of the process connecting the theoretical pseudo-receptors to the assays were simplified to a single connection because, in general, we do not know the intermediate details of these processes or even the identity of the pseudo-receptors. Note that the pseudo-receptors are conceptualized here as surrogates for generic processes such as cytotoxicity that can lead to non-ER mediated assay activity. It is possible to describe many possible alternative assay interference pathways, but in general, the current data are not sufficient to distinguish between alternate models. Pseudo-receptors are then assigned to each group of assays (technology group) and to each assay individually. Only a single example of an assay-specific pseudo-receptor is shown in Figure 1, but all assays (with the exception of A16/R8 where the assay and the receptor are identical) have a corresponding pseudo-receptor. The bottom panel of Figure 1 shows the pattern of activity one would expect if specific receptors are activated, in this case R1, R2 and R6.

Mathematical Representation of the Network Model: The computational model assumes that the value (the efficacy, A) returned by an assay at a given concentration is a linear sum of the contributions from the receptors that it measures, i.e. it is a simple linear additive model:

$$A_i = \sum_{j=1}^{N_{\text{Receptor}}} F_{ij} R_j \tag{2}$$

where the elements of the F matrix are 1 if there is a connection between a receptor j and an assay i and 0 otherwise. The index i goes over all assays and the index j goes over all receptors. This holds for direct connections, where a receptor is directly linked to an assay in Figure 1, and for indirect connections, where a receptor is linked through one or more internal nodes, designated by the circles in Figure 1. Therefore, the model assumes lossless transmission of signals from the receptor through the internal nodes to the assays. The goal is then to find a set of R_j values that minimize the difference between the predicted assay values (A_i^{pred}) and the measured ones (A_i^{meas}) for each chemical and concentration. A_i^{pred} is calculated using the forward model (Equation 2). For each chemical-concentration pair, a constrained least-squares minimization approach is used where the function being minimized is:

$$\varepsilon^2 = \sum_{i=1}^{N_{Assay}} (A_i^{pred} - A_i^{meas})^2 + \text{penalty}(R) \quad (3)$$

where A_i^{pred} must satisfy the constraints:

$$A_i^{pred} \in [0, 1]. \quad (4)$$

It is possible to assign weights to the assays in the sum of Equation 3, but in practice, this did not change the results in any qualitative way, and introduced a number of additional free parameters into the model. The term $\text{penalty}(R)$ penalizes solutions that predict that many receptors are being simultaneously activated by the chemical. It is given by

$$\text{penalty}(R) = \alpha \frac{x^{10}}{x^{10} + 0.5^{10}} \quad (5)$$

where $x = \sum_{i=1}^{N_{Receptor}} R_i$

This penalty term helps stabilize the solutions and enforces a reasonable physical assumption about chemical promiscuity, e.g., it is unlikely that many or most chemicals will selectively interact with a number of dissimilar molecular targets through non-covalent binding. Note that this problem is underdetermined because there are more receptors than assays, and so does not have a unique solution. We investigated two other commonly used penalty terms, RIDGE(Hoerl and Kennard 1970) and LASSO (Tibshirani 1996) as described in Supplemental File S1, Appendix 2. The penalty term in Equation 5 (called THRESHOLD) was selected because it best enforced the physical constraint, and because results were less sensitive to the exact value of α . For most results, we use an

intermediate value of $\alpha=1$, but the final data files additionally give selected values for $\alpha=0.01$ and $\alpha=100$. The penalized least-squares solution to Equation 3 is carried out using the R-language function *optim* in package *stats* (Ihaka and Gentleman 1996) , with method= L-BFGS-B and the constraints in Equation 4. When solving the equations, we start from the low concentration end where the expected activity is zero and use this as the initial condition for all receptors in the model. For subsequent concentrations, we then use the output values for the previous concentration as the initial values for the current one. The model results in a response value (between 0 and 1) for each receptor at each concentration. The activity for each receptor is summarized as an area under the curve (AUC), which is the integral across the concentration range:

$$AUC(R_j) = \frac{1}{N_{conc}} \sum_{i=1}^{N_{conc}} sign(slope) \times R_j(conc_i) . \tag{6}$$

The factor *sign(slope)* is included to handle cases where one of the assays or sets of assays is active at significantly lower concentrations than the remaining assays. The corresponding receptor curve will then rise and subsequently fall, and this AUC needs to be discounted. Finally, AUC values are scaled so that AUC(agonist)=1 for 17 α -Ethinylestradiol, which is the positive reference compound for all agonist assays. AUC(R1/agonist) and AUC(R2/antagonist) (or subsequently AUC(agonist)/AUC(antagonist)) is the terminology used to describe the activity in the agonist and antagonist modes, respectively. AUC(R_i; i>2) describes activity in one of the other pseudo-receptors 3-9. AUC(A_i) describes the AUC value for one of the single-assay pseudo-receptors.

One challenge with this modeling approach is how to interpret the AUC values. For a pure ER agonist (no activity in any of the pseudo-receptors), the AUC(agonist) vs. concentration curve closely resembles the concentration-response profile for any of the assays, with activity going from 0 to 1 with an AC50-like value close to that observed in the assays. For mixed cases, the concentration-response curves may be more complex than a Hill curve and will have a maximum efficacy of less than 1. Qualitatively, we interpret these AUC values as concentration-specific probabilities that the chemical is interacting with the corresponding (pseudo) receptor. One final set of quantities calculated are the “median-AC50” values. These are the median values of the log-AC50 for assays active for that chemical.

Results

Observed Correlation Among In Vitro Assays From the Same Technology: Two-dimensional hierarchical clustering was performed on the relative potencies of the 18 ER-

related *in vitro* assays (Figure 2). Strong clustering by technology / pseudo-receptor was observed. This indicates that some fraction of positive assay responses are caused by technology-specific assay interference rather than ER receptor-mediated activity. Other chemicals showed activity across a broad range of ER-related *in vitro* assays.

Network Modeling of In Vitro Assay Activity: Figure 3 illustrates common types of assay activity and model behavior represented by prototype chemicals. For example, bisphenol A (BPA) shows a clear concentration-response in agonist activity (right-hand panel, blue curve). However, there is also activity in the R6 pseudo-receptor (corresponding to the transactivation assays) that rises at low concentrations and then drops. The corresponding *in vitro* assays show activity at lower concentrations than the others, but at high concentrations, substantial evidence points toward agonist activity. Note that BPA also has activity in one of the antagonist assays (upper left panel, A17, gold line), consistent with known SERM activity at high concentrations (Nagel, Hagelbarger et al. 2001). 4-hydroxytamoxifen, a reference antagonist, shows clear antagonist activity. Alpha-cyclodextrin shows strong activity only in the three cell-free binding assays, resulting in a strong assay interference signal in the R3 pseudo-receptor. This is likely because this chemical interferes with the radioligand assay by binding to the radioligand. This molecule is known to bind hydrophobic molecules such as fatty acids and cholesterol (Christian, Haynes et al. 1997). The most frequent case (not shown here) is one in which there is no activity in any assay. The data for the complete set of chemicals are given in Supplemental Files S2 (tabular) and S3 (plots corresponding to Figure 3).

Reference Chemicals: The AUC values for the ER reference chemicals are plotted in Figure 4. For the positive agonist chemicals, all but diethylhexyl phthalate (DEHP) and dicofol have non-zero AUC(agonist) values. DEHP is inactive in all assays, but dicofol is active in 3 of the 6 dimerization assays near the top of the tested concentration range, which results in a small but non-zero AUC(R4) value of 0.02. These two chemicals are in the “Very Weak” class, so they are potentially active only at concentrations above where the current assays have been tested for most or all assays (100 μ M). The AUC(agonist) values for the other positive chemicals are ordered approximately with the expected potency class. All of the negative agonist reference chemicals showed AUC(agonist) values of zero.

All four of the positive antagonist reference chemicals are positive with large AUC(antagonist) values. Three negative antagonist reference chemicals yield non-zero AUC(antagonist), but all are <0.05 . Most of the negative antagonist reference chemicals are positive references for the agonist mode, and they appropriately yield a high

AUC(agonist) value. A specific example is dibutyl phthalate, which is defined in the OECD reference list as a very weak positive agonist and a negative antagonist. Our data shows very weak activity in both modes, however, all activity occurs in the cytotoxicity region (see the inset in the figure). Therefore, the activity in the antagonist assays leading to the non-zero AUC(antagonist) may be driven by false-positive loss of signal due to cytotoxicity. In general, we see that the positive reference chemicals, with the exception of some that are very weak, are classified as having the appropriate activity class (i.e., agonist or antagonist). Negative reference chemicals either have no activity in any assay or are classed as being active in only one of the pseudo-receptor channels with scores higher than for the agonist or antagonist receptors. Supplemental File S4 provide the agonist and antagonist mode AUC values for the reference chemicals and plots of the assay and receptor concentration-response profiles, respectively.

Activity Classifications of the Commercial and Environmental Chemicals: Figure 5 summarizes the results of the modeling effort over the 1812 chemicals. In the idealized case where all assays are activated (either relevant for the agonist or antagonist mode) at the same concentration, and reach 100% efficacy, the relation between the median-AC50 (which would be the common AC50 for all assays) and AUC would be linear. However, in the more common case where the assay AC50s are spread out, the agonist / antagonist curve tends to rise sooner than the median of the assays (See Figure 3 for BPA comparing the blue agonist curve with the assays AC50 median, the green vertical line). The dashed line is the best fit from a liner regression between AUC and $\log(\text{minimum-AC50})$ for chemicals with $\text{AUC} > 0.1$. The horizontal line at $\text{AUC} = 0.1$ provides a qualitative break between chemicals following the linear AC50 vs. AUC trend and those showing low potency in one or a few assays.

Chemicals fall into one of several general groups. The first are those lying along the dashed line, which is the expected behavior for true actives. We have labeled the most potent non-reference chemicals, those with $\text{AUC} > 0.4$ (chemicals 1-10). Fulvestrant, equilin, estriol, clomiphene citrate, and mestranol are all steroid pharmaceuticals that are designed to target ER (Wishart, Knox et al. 2008). Bisphenol AF is a close analog of bisphenol A, one of the reference agonist chemicals. Zearalenone is a mycotoxin with known estrogenic activity (Le Guevel and Pakdel 2001, Higa-Nishiyama, Takahashi-Ando et al. 2005). HPTE is a degradate of the pesticide methoxychlor and is a known environmental estrogen (Miller, Gupta et al. 2006). Norethindrone is a progesterone derivative. 17beta-Trenbolone is synthetic androgen. Both of these steroids appear to be weakly active against ER relative to their activity in their native receptor. Therefore, none of the most potent set of actives is novel.

1
2
3
4
5
6
7
8
9
10
11
12
13
14
15
16
17
18
19
20
21
22
23
24
25
26
27
28
29
30
31
32
33
34
35
36
37
38
39
40
41
42
43
44
45
46
47
48
49
50
51
52
53
54
55
56
57
58
59
60

A second interesting set of chemicals are those labeled in cyan in (chemicals 11-13). These have low but significant AUC values (0.1-0.2) but have at least one very potent AC50 value. The most potent of these is 4-androstene-3,17-dione, a potent androgen. The assay plot for this chemical is shown as an inset in Figure 5. The most potent assays are the ATG transactivation assays. This assay platform has two interesting features, first that it is run in HepG2 cells with some metabolic activity, and second, that it is highly multiplexed, including having androgen receptor readouts simultaneous with those for the estrogen receptor. So, two possibilities exist for the potent activity of this androgen - there could be metabolic activation, leading to real ER activity, or there could be assay technology crosstalk. Understanding this behavior is the subject of ongoing research. Melengestrol acetate is progestin, and is most potent in the ACEA cell proliferation assay. The cells used in the proliferation assay (T47D) are known to be sensitive to progestins and glucocorticoids (Chan, Klock et al. 1989). 3,3'-Dimethylbenzidine dihydrochloride, an intermediate in the production of dyes, is active in the 3 cell-free radioligand binding assays, indicating its potential to disrupt the protein in these assays, potentially through protein denaturation.

A final set of chemicals are those with some weak activity in one or more of the assays. There are further chemicals with AUC(agonist) in the range of values seen with the weak and very weak reference chemicals (green triangles, lower right of figure), and these would be worth additional investigation, although with a lower priority than those chemicals that are more potent. Note that there is greater uncertainty about activity for chemicals where the "true" activity approaches the upper limit of testing (100 μ M) because of the large spread in AC50 values across the assays. Finally, there are a set of chemicals with very low median-AC50, but low or zero AUC(agonist/antagonist) (black points running along the bottom middle). These chemicals are very potent in one assay or technology, and are the typical chemicals causing assay interference.

One goal of this study was to determine whether a chemical interacts with ER based on data from *in vitro* assay which is subject to noise and assay interference. Table 2 gives the counts of chemicals for each of the receptors or pseudo-receptors with at least one chemical having an AUC>0.2, over selected ranges. For the agonists and antagonists, one can see that the number of chemicals in these potency categories shifts as a function of the penalty term strength α (see Equation 5).

Understanding all of the causes of assay interference (and hence pseudo-receptor activity) is beyond the scope of this study, but we analyzed two major factors that appear to play a role in our study. These factors include non-normal baseline variability and cytotoxicity or cell-stress-induced non-specific activity. In the assay data processing pipeline (see Methods), baseline variability is assumed to be approximately normally

distributed, and to be due to noise processes. However, other processes can cause baseline shifts, for instance uncorrected edge effects on a microtiter plate. Assay data processing attempts to correct for these types of effects, but in a high-throughput automated system, some issues will remain. To be called a hit in our current data analysis process, the maximum efficacy (T/Top) must be above a defined statistical criteria, which is typically 10 MAD (median absolute deviation, essentially 10 standard deviations) above baseline. Given this relatively high threshold, one would expect few noise-related false positives if the noise was approximately normally distributed. A second potential cause of assay interference is cell-stress or cytotoxicity related non-selective activity. With *in vitro* assays, one often observes false activity in many assays at concentrations near cytotoxicity. We term this phenomenon the cytotoxicity “burst”. The Z-score (see methods) is used to quantify the relative proximity of an assay AC50 to the cytotoxicity region. Qualitatively, $Z < 3$ may be associated with cytotoxicity, while $Z \geq 3$ is not. For most assays, we observe a bimodal distribution of Z-scores with a minimum at ~ 3 . An example of the Z-score distribution is shown in Figure 6 for ATG_ERa_TRANS_up (assay A12).

For subsequent analyses, we examined chemical activity after filtering for likely non-ER activity using maximum efficacy (Top or T) and cytotoxicity (i.e., Z-score). For each chemical, the median T and Z-scores were calculated for the corresponding assays, and chemicals were removed with $T < 50\%$ or $Z < 3$. A total of 165 chemicals passed this filter. The chemicals filtered out typically those with low AUC values (active only at high concentrations). Figure 7 shows the fraction of chemicals remaining after the filtering for receptors or pseudo-receptors with more than 5 hits and with $AUC > 0.1$ before filtering. For illustration, only multi-assay pseudo-receptors are shown. One can see that the low AUC bins lose the most number of chemicals. Pseudo-receptor R9 loses the largest fraction of chemicals in all bins, likely because the loss-of-signal antagonist assays making up R9 are the most subject to being confounded by cytotoxicity. This is in contrast to R3, made up of the cell-free radioligand binding assays, which lose the smallest fraction of chemicals in the intermediate AUC bins, likely because these assays are less sensitive to the cytotoxicity processes. Finally, note that a number of agonist and antagonist chemicals in the low and intermediate AUC bins are also lost. These are chemicals that have many assays active, and include some of known weak estrogens (linear nonylphenol is an example), but whose activity all occurs in the cytotoxicity region. We would argue that, while these chemicals may be truly estrogenic, they are of more concern from their cytotoxicity than as estrogens.

A total of 72 chemicals have an AUC(agonist) or AUC(antagonist) > 0.1 , median-Z-score > 3 , and median-T $> 50\%$. These are listed, along with a variety of annotations in Table 3. Many of these chemicals fall into two main structural classes with known

estrogenic activity - steroids (16, 22%), and phenol-containing compounds (41, 57%). Pharmaceuticals are the most widely represented use class (28, 39%). Other use classes include antioxidants, detergents/surfactants, pesticides, plastics and other industrial reagents and UV absorbers. Another interesting class are chemicals that are found in foods, including the natural phytoestrogen flavones genistein, daidzein, biochanin A, apigenin, kaempferol and chrysin; and the flavor / fragrance ingredient 4-(2-methylbutan-2-yl)cyclohexanol (also known as 4-tert-amylcyclohexanol), which is a perfume ingredient.

Discussion

We have developed a computational approach to distinguish true ER receptor-mediated agonist and antagonist activity from false positive activity often related, we postulate, to assay interference. The primary driver of this application is the need to screen thousands of man-made chemicals found in the environment for their potential to interact with the estrogen receptor. Current *in vivo* methods used for chemical safety testing are too slow and resource intensive to screen a set of chemicals of this magnitude. The present method ranks large numbers of chemicals based on potential ER pathway activity in a way that is useful for setting priorities for further screening or testing.

The method described here uses a network model to integrate concentration-response profiles for a collection of 18 *in vitro* assays probing different molecular processes in the ER pathway. The model assigns scores for true agonist and antagonist activity as well as scores representing non-receptor mediated effects. Model scores are combined with a measure of relative efficacy and cytotoxicity-related assay activity. These results indicate whether the activity of a chemical is most likely ER mediated, or related to either assay- or technology-specific assay interference. Model results demonstrate that the method works well for a set of reference chemicals and correctly identifies agonist, antagonist and inactive compounds with high sensitivity and specificity. The model agonist score [AUC(agonist)] is also correlated with the expected potency class of the active reference chemicals.

Additionally, this study allowed us to probe mechanisms behind assay interference. The existence of this phenomenon is well known in the pharmaceutical industry, and some models to identify interfering chemicals are available (Baell and Holloway 2010, Bruns and Watson 2012). However, we believe that the types of interference one sees may indicate important aspects of the underlying biology triggered by these chemicals, although typically only at high concentrations. We have demonstrated here that a fraction of pseudo-receptor activity is associated with cytotoxicity, but the phenomenon of cytotoxicity is not uniform. In particular, Figure 7

shows that the chemicals with lower support for activity against any of the receptors or pseudo-receptors (as measured by AUC values) are the ones most likely to have assay activity occurring only in the cytotoxicity region. In the ToxCast assay portfolio, a total of 35 cytotoxicity assays are run in multiple cell types (cell lines and primary cells), and different types of readouts (primarily measuring decrease in viable cell count, ATP levels or decrease in rate of cell proliferation). We observed (data not shown) that many chemicals will trigger only one class of the cytotoxicity assays in the burst region (e.g., only the cell-line-based assays, or only the reduced proliferation assays), indicating the potential for a specific mechanism for cytotoxicity. The ToxCast assay portfolio also contains a collection of cell stress assays (e.g., oxidative stress, endoplasmic reticulum stress, mitochondrial disruption). We are currently studying how to combine patterns of assay interference, cell stress and cytotoxicity with the aim of better understanding how chemicals perturb cells at high concentrations. Understanding these effects may also help interpret the results of typical high-dose animal toxicity studies as many of these effects are dose-dependent.

As the network modeling performed in this study relies solely on *in vitro* determinations of activity, equally important is the need for high-throughput quantitative estimations of pharmacokinetics (Rotroff, Wetmore et al. 2010, Wetmore, Wambaugh et al. 2012, Thomas, Philbert et al. 2013, Wetmore, Wambaugh et al. 2013) and chemical exposure (Wambaugh, Setzer et al. 2013, Wambaugh, Wang et al. 2014). This will provide the capability to develop risk-based priorities for targeted testing within the framework of high-throughput risk assessment (Judson, Kavlock et al. 2011). In addition, the method described here is general enough to apply to any pathway for which multiple assays are available that probe different points in a pathway using multiple technologies. We currently have equivalent data sets to the one described here for the androgen receptor, steroidogenesis, and the peroxisome proliferator activating receptor (PPAR) pathways (ref needed). We are also adding physico-chemical properties and other structural features to try and develop rules to be used in designing safer alternatives to currently widely used chemicals. The estrogen receptor context is helpful in this broad area because we can better assess what is true receptor-mediated activity as opposed to assay interference. We can likely apply assay interference information for specific chemicals derived from this ER study to the behavior of those chemicals in other pathways, for which we do not have this large assay coverage.

Supplementary Data Description:

Four supplemental files are provided:

- S1 SUPPLEMENTAL ER pathway model 2015-04-08.docx: This provides further details on the experimental protocols (in vitro assays), and information on sensitivity analysis for the model

- S2 ER SuperMatrix 2015-03-24.xlsx: Spreadsheet with all input and output data and model parameters the 1800 chemicals
- S3 AUC plots for all chemicals 2015-03-24 THRESHOLD 1.pdf: plots for all chemicals similar to the examples shown in Figure 3.
- S4 AUC plots for reference chemicals 2015-03-24 THRESHOLD 1.pdf: plots for the ER reference chemicals similar to the examples shown in Figure 3.

Additionally, the software used to run the model and all input and output data will be provided as a zip file on the authors' web site: <http://epa.gov/ncct/toxcast/data.html>.

Funding Information

The authors gratefully acknowledge the American Institute of Mathematics and National Science Foundation for support of this research through the "Modeling Problems Related to Our Environment" workshop held January 14-18, 2013 in Palo Alto CA. All other funding was provided by the U.S. EPA.

References

Akaike, H. (1998). Information theory and an extension of the maximum likelihood principle. New York, Springer.

Auld, D. S., N. Thorne, D. T. Nguyen and J. Inglese (2008). "A specific mechanism for nonspecific activation in reporter-gene assays." ACS Chem Biol **3**(8): 463-470.

Baell, J. B. and G. A. Holloway (2010). "New substructure filters for removal of pan assay interference compounds (PAINS) from screening libraries and for their exclusion in bioassays." J Med Chem **53**(7): 2719-2740.

Bruns, R. F. and I. A. Watson (2012). "Rules for identifying potentially reactive or promiscuous compounds." J Med Chem **55**(22): 9763-9772.

Chan, W. K., G. Klock and H. U. Bernard (1989). "Progesterone and glucocorticoid response elements occur in the long control regions of several human papillomaviruses involved in anogenital neoplasia." J Virol **63**(8): 3261-3269.

Christian, A. E., M. P. Haynes, M. C. Phillips and G. H. Rothblat (1997). "Use of cyclodextrins for manipulating cellular cholesterol content." J Lipid Res **38**(11): 2264-2272.

Diel, P., S. Olff, S. Schmidt and H. Michna (2001). "Molecular identification of potential selective estrogen receptor modulator (SERM) like properties of phytoestrogens in the human breast cancer cell line MCF-7." Planta Med **67**(6): 510-514.

Dix, D. J., K. A. Houck, M. T. Martin, A. M. Richard, R. W. Setzer and R. J. Kavlock (2007). "The ToxCast program for prioritizing toxicity testing of environmental chemicals." Toxicol. Sci. **95**(1): 5-12.

Dutertre, M. and C. L. Smith (2000). "Molecular mechanisms of selective estrogen receptor modulator (SERM) action." J Pharmacol Exp Ther **295**(2): 431-437.

Filer, D. L. (2015). "In Preparation."

Gronemeyer, H., J. A. Gustafsson and V. Laudet (2004). "Principles for modulation of the nuclear receptor superfamily." Nat Rev Drug Discov **3**(11): 950-964.

Higa-Nishiyama, A., N. Takahashi-Ando, T. Shimizu, T. Kudo, I. Yamaguchi and M. Kimura (2005). "A model transgenic cereal plant with detoxification activity for the estrogenic mycotoxin zearalenone." Transgenic Res **14**(5): 713-717.

Hoerl, A. E. and R. W. Kennard (1970). "Ridge Regression: Biased estimation for nonorthogonal problems." Technometrics **12**(1): 55-67.

Huang, R., S. Sakamuru, M. T. Martin, D. M. Reif, R. S. Judson, K. A. Houck, W. Casey, J. H. Hsieh, K. R. Shockley, P. Ceger, J. Fostel, K. L. Witt, W. Tong, D. M. Rotroff, T. Zhao, P. Shinn, A. Simeonov, D. J. Dix, C. P. Austin, R. J. Kavlock, R. R. Tice and M. Xia (2014). "Profiling of the Tox21 10K compound library for agonists and antagonists of the estrogen receptor alpha signaling pathway." Sci Rep **4**: 5664.

Ihaka, R. and R. Gentleman (1996). "R: A language for data analysis and graphics." J.Comput and Graphical Statistics **5** 299-314.

Judson, R. S., K. A. Houck, R. J. Kavlock, T. B. Knudsen, M. T. Martin, H. M. Mortensen, D. M. Reif, D. M. Rotroff, I. Shah, A. M. Richard and D. J. Dix (2010). "In vitro screening of environmental chemicals for targeted testing prioritization: the ToxCast project." Environ Health Perspect **118**(4): 485-492.

Judson, R. S., R. J. Kavlock, R. W. Setzer, E. A. Cohen Hubal, M. T. Martin, T. B. Knudsen, K. A. Houck, R. S. Thomas, B. A. Wetmore and D. J. Dix (2011). "Estimating toxicity-related biological pathway altering doses for high-throughput chemical risk assessment." Chem Res Toxicol **24**(4): 451-462.

Katzenellenbogen, B. S., I. Choi, R. Delage-Mourroux, T. R. Ediger, P. G. Martini, M. Montano, J. Sun, K. Weis and J. A. Katzenellenbogen (2000). "Molecular mechanisms of estrogen action: selective ligands and receptor pharmacology." J Steroid Biochem Mol Biol **74**(5): 279-285.

Katzenellenbogen, B. S. and J. A. Katzenellenbogen (2000). "Estrogen receptor transcription and transactivation: Estrogen receptor alpha and estrogen receptor beta: regulation by selective estrogen receptor modulators and importance in breast cancer." Breast Cancer Res **2**(5): 335-344.

Katzenellenbogen, B. S., M. M. Montano, T. R. Ediger, J. Sun, K. Ekena, G. Lazennec, P. G. Martini, E. M. McInerney, R. Delage-Mourroux, K. Weis and J. A. Katzenellenbogen (2000). "Estrogen receptors: selective ligands, partners, and distinctive pharmacology." Recent Prog Horm Res **55**: 163-193; discussion 194-165.

Kavlock, R., K. Chandler, K. Houck, S. Hunter, R. Judson, N. Kleinstreuer, T. Knudsen, M. Martin, S. Padilla, D. Reif, A. Richard, D. Rotroff, N. Sipes and D. Dix (2012). "Update on EPA's ToxCast program: providing high throughput decision support tools for chemical risk management." Chem Res Toxicol **25**(7): 1287-1302.

Knudsen, T. B., K. A. Houck, N. S. Sipes, A. V. Singh, R. S. Judson, M. T. Martin, A. Weissman, N. C. Kleinstreuer, H. M. Mortensen, D. M. Reif, J. R. Rabinowitz, R. W. Setzer, A. M. Richard, D. J. Dix and R. J. Kavlock (2011). "Activity profiles of 309 ToxCast chemicals evaluated across 292 biochemical targets." Toxicology **282**(1-2): 1-15.

Le Guevel, R. and F. Pakdel (2001). "Assessment of oestrogenic potency of chemicals used as growth promoter by in-vitro methods." Hum Reprod **16**(5): 1030-1036.

Mangelsdorf, D. J., C. Thummel, M. Beato, P. Herrlich, G. Schutz, K. Umesono, B. Blumberg, P. Kastner, M. Mark, P. Chambon and R. M. Evans (1995). "The nuclear receptor superfamily: the second decade." Cell **83**(6): 835-839.

Martin, M. T., D. J. Dix, R. S. Judson, R. J. Kavlock, D. M. Reif, A. M. Richard, D. M. Rotroff, S. Romanov, A. Medvedev, N. Poltoratskaya, M. Gambarian, M. Moeser, S. S. Makarov and K. A. Houck (2010). "Impact of environmental chemicals on key transcription regulators and correlation to toxicity end points within EPA's ToxCast program." Chem Res Toxicol **23**(3): 578-590.

Miller, J. R., V. Thanabal, M. M. Melnick, M. Lall, C. Donovan, R. W. Sarver, D. Y. Lee, J. Ohren and D. Emerson (2010). "The use of biochemical and biophysical tools for triage of high-throughput screening hits - A case study with Escherichia coli phosphopantetheine adenylyltransferase." Chem Biol Drug Des **75**(5): 444-454.

Miller, K. P., R. K. Gupta and J. A. Flaws (2006). "Methoxychlor metabolites may cause ovarian toxicity through estrogen-regulated pathways." Toxicol Sci **93**(1): 180-188.

Nagel, S. C., J. L. Hagelbarger and D. P. McDonnell (2001). "Development of an ER action indicator mouse for the study of estrogens, selective ER modulators (SERMs), and Xenobiotics." Endocrinology **142**(11): 4721-4728.

OECD (2012). OECD Test No. 457: BG1Luc Estrogen Receptor Transactivation Test Method for Identifying Estrogen Receptor Agonists and Antagonists. **2012**.

Reif, D. M., M. T. Martin, S. W. Tan, K. A. Houck, R. S. Judson, A. M. Richard, T. B. Knudsen, D. J. Dix and R. J. Kavlock (2010). "Endocrine profiling and prioritization of

environmental chemicals using ToxCast data." Environ Health Perspect **118**(12): 1714-1720.

Rotroff, D. M., D. J. Dix, K. A. Houck, R. J. Kavlock, T. B. Knudsen, M. T. Martin, D. M. Reif, A. M. Richard, N. S. Sipes, Y. A. Abassi, C. Jin, M. Stampfl and R. S. Judson (2013). "Real-Time Growth Kinetics Measuring Hormone Mimicry for ToxCast Chemicals in T-47D Human Ductal Carcinoma Cells." Chem Res Toxicol **26**(7): 1097-1107.

Rotroff, D. M., M. T. Martin, D. J. Dix, D. L. Filer, K. A. Houck, T. B. Knudsen, N. S. Sipes, D. M. Reif, M. Xia, R. Huang and R. S. Judson (2014). "Predictive endocrine testing in the 21st century using in vitro assays of estrogen receptor signaling responses." Environ Sci Technol **48**(15): 8706-8716.

Rotroff, D. M., B. A. Wetmore, D. J. Dix, S. S. Ferguson, H. J. Clewell, K. A. Houck, E. L. Lecluyse, M. E. Andersen, R. S. Judson, C. M. Smith, M. A. Sochaski, R. J. Kavlock, F. Boellmann, M. T. Martin, D. M. Reif, J. F. Wambaugh and R. S. Thomas (2010). "Incorporating human dosimetry and exposure into high-throughput in vitro toxicity screening." Toxicol Sci **117**(2): 348-358.

Sipes, N. S., M. T. Martin, P. Kothiya, D. M. Reif, R. S. Judson, A. M. Richard, K. A. Houck, D. J. Dix, R. J. Kavlock and T. B. Knudsen (2013). "Profiling 976 ToxCast chemicals across 331 enzymatic and receptor signaling assays." Chem Res Toxicol **26**(6): 878-895.

Thomas, R. S., M. A. Philbert, S. S. Auerbach, B. A. Wetmore, M. J. Devito, I. Cote, J. C. Rowlands, M. P. Whelan, S. M. Hays, M. E. Andersen, M. E. Meek, L. W. Reiter, J. C. Lambert, H. J. Clewell, 3rd, M. L. Stephens, Q. J. Zhao, S. C. Wesselkamper, L. Flowers, E. W. Carney, T. P. Pastoor, D. D. Petersen, C. L. Yauk and A. Nong (2013). "Incorporating new technologies into toxicity testing and risk assessment: moving from 21st century vision to a data-driven framework." Toxicol Sci **136**(1): 4-18.

Thorne, N., D. S. Auld and J. Inglese (2010). "Apparent activity in high-throughput screening: origins of compound-dependent assay interference." Curr Opin Chem Biol **14**(3): 315-324.

Tibshirani, R. (1996). "Regression shrinkage and selection via the Lasso." Journal of the Royal Statistical Society Series B-Methodological **58**(1): 267-288.

Wambaugh, J. F., R. W. Setzer, D. M. Reif, S. Gangwal, J. Mitchell-Blackwood, J. A. Arnot, O. Joliet, A. Frame, J. Rabinowitz, T. B. Knudsen, R. S. Judson, P. Egeghy, D. Vallero and E. A. Cohen Hubal (2013). "High-throughput models for exposure-based chemical prioritization in the ExpoCast project." Environ Sci Technol **47**(15): 8479-8488.

Wambaugh, J. F., A. Wang, K. L. Dionisio, A. Frame, P. Egeghy, R. Judson and R. W. Setzer (2014). "High throughput heuristics for prioritizing human exposure to environmental chemicals." Environ Sci Technol **48**(21): 12760-12767.

Wetmore, B. A., J. F. Wambaugh, S. S. Ferguson, L. Li, H. J. Clewell, 3rd, R. S. Judson, K. Freeman, W. Bao, M. A. Sochaski, T. M. Chu, M. B. Black, E. Healy, B. Allen, M. E. Andersen, R. D. Wolfinger and R. S. Thomas (2013). "Relative impact of incorporating pharmacokinetics on predicting in vivo hazard and mode of action from high-throughput in vitro toxicity assays." *Toxicol Sci* **132**(2): 327-346.

Wetmore, B. A., J. F. Wambaugh, S. S. Ferguson, M. A. Sochaski, D. M. Rotroff, K. Freeman, H. J. Clewell, 3rd, D. J. Dix, M. E. Andersen, K. A. Houck, B. Allen, R. S. Judson, R. Singh, R. J. Kavlock, A. M. Richard and R. S. Thomas (2012). "Integration of dosimetry, exposure, and high-throughput screening data in chemical toxicity assessment." *Toxicol Sci* **125**(1): 157-174.

Wishart, D. S., C. Knox, A. C. Guo, D. Cheng, S. Shrivastava, D. Tzur, B. Gautam and M. Hassanali (2008). "DrugBank: a knowledgebase for drugs, drug actions and drug targets." *Nucleic Acids Res* **36**(Database issue): D901-906.

Figure Legends:

Figure 1: (A) Graphical representation of the computational network used in the *in vitro* analysis of the ER pathway across assays and technology platforms. Colored arrow nodes represent "receptors" with which a chemical can directly interact. Colored circles represent intermediate biological processes that are not directly observable. White stars represent the *in vitro* assays that measure activity at the biological nodes. Arrows represent transfer of information. Gray arrow nodes are the pseudo-receptors. Each *in vitro* assay (with the exception of A16) has an assay-specific pseudo-receptor, but only a single example is explicitly shown, for assay A1. (B) Patterns of assays that would be activated when specific receptors are activated by the chemical, in particular R1, R2 and R6. The activating chemical in its receptor are circled in pink, and the activated assays and the pathways to them are also highlighted in pink.

Figure 2: Two-way hierarchical clustering of chemical activity across the 18 *in vitro* assays used to test for ER activity. The heatmap shows $-\log_{10}(\text{AC}_{50})$ values for all assays and all chemicals with at least one assay hit. Darker red indicates more potent activity (lower AC_{50}), while white represents inactive chemical-assay pairs. Note that the assays cluster by technology / pseudo-receptor. The "A" and "R" values refer to the assay and receptors/pseudo-receptors from Figure 1 and Table 1.

Figure 3: Results of the model for three prototype chemicals. For each chemical, the left-hand panel shows the synthetic concentration-response data for the 18 assays, colored by assay group defined the legend. The right-hand panel shows the corresponding magnitude

of the modeled receptor responses. The agonist receptor (R1) is designated by blue, the antagonist receptor (R2) by red and the other pseudo-receptors are colored as indicated in the legend. AUC values for the agonist (R1) and antagonist (R2) receptors are provided below the chemical name. For chemicals with the cytotoxicity burst defined (2 or more cytotoxicity hits, see Methods), the burst center is indicated by a vertical red line, and the burst region (starting 3 burst MAD below the burst center) is indicated by the gray shaded region. A green horizontal bar indicates the median-AC50 of the active assays. Similar plots for all chemicals are given in Supplemental File S3.

Figure 4: Plots showing activity of the agonist (top) and antagonist (bottom) reference chemicals. Chemicals that are intended to be positive are indicated by green circles, while those intended to be inactive are indicated by red circles. For the agonists, the expected potency range is also indicated (middle column). For chemicals with one or more pseudo-receptor AUC values greater than zero, the value is indicated by an X, and the pseudo-receptor name is indicated. The inset shows the assay curves for dibutyl phthalate, as described in the text (colored based on Figure 3).

Figure 5: Plot of the maximum AUC vs. minimum-AC50 values. Each point is a single chemical that was active in at least one assay. The AUC value given is the maximum of the AUC(agonist) and AUC(antagonist) values for the chemical. The dashed line is the best-fit for AUC(agonist) values >0.1. Chemicals are labeled in order: black circle, at least one AUC>0.1; green up-arrow, positive agonist reference chemical; green down-arrow, positive antagonist reference chemical; red diamond, negative reference chemical; cyan circle, example chemicals with AUC significantly below the fitted line but above 0.1. The vertical line at 100 μ M indicates the highest concentration tested, while the horizontal line at AUC=0.1 indicates an approximate threshold between chemicals with clear agonist / antagonist activity and those that are potentially active through interference processes. The inset shows graphs of assay activity for 4-androstene-3,17-dione (colored based on Figure 3).

Figure 6: Histogram of Z-scores for the assay ATG_ERa_TRANS_up. The Z-score is defined as the distance between the median cytotoxicity concentration and a chemical's AC50 in this assay, in units of global cytotoxicity MAD, for all chemicals active in this assay. One can see a bimodal distribution with one peak at zero (marked with a heavy red line) and another with a peak near 6. We hypothesize that chemicals active in the low-Z region are more likely to be false positives and less likely to be estrogenic than those active in the high-Z region.

Figure 7: Bar chart showing the fraction of chemicals remaining for each of the multi-assay receptors / pseudo-receptors after filtering for efficacy (T) and cytotoxicity (Z-score). The receptors were limited to those with 5 or more chemicals with AUC>0.1 from Table 2. If there were no chemicals for a pseudo-receptor in a given AUC bin, a small negative bar is shown. The legend indicates AUC ranges corresponding to Table 2.

1
2
3
4
5
6
7
8
9
10
11
12
13
14
15
16
17
18
19
20
21
22
23
24
25
26
27
28
29
30
31
32
33
34
35
36
37
38
39
40
41
42
43
44
45
46
47
48
49

Tables

Table 1: Summary of the *in vitro* assays used with their ID mapping to the model in Figure 1. Further details are provided in Supplemental File S1, Appendix 1. NVS=Novascreen; OT=Odyssey Thera; ATG=Attagene; Tox21=assays run by the National Institutes of Health’s National Center for Advancing Translational Sciences (NCATS) as part of the Federal Tox21 program.

Assay ID	Assay Name	Source	GeneTarget	Normalized Data Type	Assay Design Type	Biological Process Target	Detection Technology	Detection Technology Subtype	Measurement Timepoint (Hours)	Organism	Tissue	Cell Format	Cell Line Name	Assay Footprint
A1	NVS_NR_bER	NVS	ESR1	percent activity	radioligand binding	receptor binding	Lysate-based radiodetection	Scintillation counting	18	bovine	uterus	tissue based cell-free	NA	microplate: 96-well plate
A2	NVS_NR_hER	NVS	ESR1	percent activity	radioligand binding	receptor binding	Lysate-based radiodetection	Scintillation counting	18	human	NA	cell-free	NA	microplate: 96-well plate
A3	NVS_NR_mERa	NVS	Esr1	percent activity	radioligand binding	receptor binding	Filter-based radiodetection	Scintillation counting	18	mouse	NA	cell-free	NA	microplate: 96-well plate
A4	OT_ER_ERaERa_0480	OT	ESR1	percent activity	protein fragment complementation assay	protein stabilization	Protein-fragment Complementation	Fluorescence intensity	8	human	kidney	cell line	HEK293T	microplate: 384-well plate
A5	OT_ER_ERaERa_1440	OT	ESR1	percent activity	protein fragment complementation assay	protein stabilization	Protein-fragment Complementation	Fluorescence intensity	24	human	kidney	cell line	HEK293T	microplate: 384-well plate
A6	OT_ER_ERaERb_0480	OT	ESR1	percent activity	protein fragment complementation assay	protein stabilization	Protein-fragment Complementation	Fluorescence intensity	8	human	kidney	cell line	HEK293T	microplate: 384-well plate

A7	OT_ER_ERaERb_1440	OT	ESR1 ESR2	percent activity	protein fragment complemen tation assay	protein stabilization	Protein- fragment Complementati on	Fluorescence intensity	24	human	kidney	cell line	HEK293T	microplate: 384-well plate
A8	OT_ER_ERbERb_0480	OT	ESR2	percent activity	protein fragment complemen tation assay	protein stabilization	Protein- fragment Complementati on	Fluorescence intensity	8	human	kidney	cell line	HEK293T	microplate: 384-well plate
A9	OT_ER_ERbERb_1440	OT	ESR2	percent activity	protein fragment complemen tation assay	protein stabilization	Protein- fragment Complementati on	Fluorescence intensity	24	human	kidney	cell line	HEK293T	microplate: 384-well plate
A10	OT_ERa_EREgFP_0120	OT	ESR1	percent activity	fluorescent protein induction	regulation of gene expression	Microscopy	Optical microscopy: Fluorescence microscopy	2	human	cervix	cell line	HeLa	microplate: 384-well plate
A11	OT_ERa_EREgFP_0480	OT	ESR1	percent activity	fluorescent protein induction	regulation of gene expression	Microscopy	Optical microscopy: Fluorescence microscopy	8	human	cervix	cell line	HeLa	microplate: 384-well plate
A12	ATG_ERa_TRANS_up	ATG	ESR1	log2 fold induction	mRNA induction	regulation of transcription factor activity	RT-PCR and Capillary electrophoresis	Fluorescence intensity	24	human	liver	cell line	HepG2	microplate: 24-well plate
A13	ATG_ERE_CIS_up	ATG	ESR1	log2 fold induction	mRNA induction	regulation of transcription factor activity	RT-PCR and Capillary electrophoresis	Fluorescence intensity	24	human	liver	cell line	HepG2	microplate: 24-well plate
A14	Tox21_ERa_BLA_Agonist_ratio	Tox21	ESR1	percent activity	beta lactamase induction	regulation of gene expression	GAL4 b- lactamase reporter gene	Fluorescence intensity	18	human	kidney	cell line	HEK293T	microplate: 1536-well plate
A15	Tox21_ERa_LUC_BG1_Agonist	Tox21	ESR1	percent activity	luciferase induction	regulation of gene expression	Luciferase- coupled ATP quantitation	Bioluminescence	22- 24	human	ovary	cell line	BG1	microplate: 1536-well plate
A16	ACEA_T47D_80hr_Positive	ACEA	ESR1	percent activity	real-time cell-growth kinetics	cell proliferation	RT-CES	Electrical Sensor: Impedance	80	human	breast	cell line	T47D	microplate: 96-well plate

A17	Tox21_ERa_BLA_Antagonist_ratio	Tox21	ESR1	percent activity	beta lactamase induction	regulation of gene expression	GAL4 b-lactamase reporter gene	Fluorescence intensity	18	human	kidney	cell line	HEK293T	microplate: 1536-well plate
A18	Tox21_ERa_LUC_BG1_Antagonist	Tox21	ESR1	percent activity	luciferase induction	regulation of gene expression	Luciferase-coupled ATP quantitation	Bioluminescence	22	human	ovary	cell line	BG1	microplate: 1536-well plate

Table 2: Counts of chemicals for each receptor/pseudo-receptor as a function of AUC value. Only receptors or pseudo receptors with at least one chemicals with AUC>0.2 are listed. Counts for the Agonist and antagonist modes as a function of α are also given. Note that for the pseudo receptors, all values use $\alpha=1$.

Receptor	0.1 to 0.2	0.2 to 0.5	0.5 to 1
AUC(Agonist) $\alpha=0.01$	22	37	12
AUC(Agonist) $\alpha=1$	36	42	14
AUC(Agonist) $\alpha=100$	51	49	16
AUC(Antagonist) $\alpha=0.01$	4	4	4
AUC(Antagonist) $\alpha=1$	9	4	5
AUC(Antagonist) $\alpha=100$	10	8	5
AUC(R3)	3	2	0
AUC(R6)	36	7	0
AUC(R7)	0	0	1
AUC(R8)	14	15	2
AUC(R9)	21	4	0
AUC(A1)	0	1	1
AUC(A2)	4	1	0
AUC(A3)	12	7	0
AUC(A12)	17	2	0
AUC(A13)	32	9	0
AUC(A15)	30	5	0
AUC(A17)	29	6	0
AUC(A18)	7	6	0

1
2
3
4
5
6
7
8
9
10
11
12
13
14
15
16
17
18
19
20
21
22
23
24
25
26
27
28
29
30
31
32
33
34
35
36
37
38
39
40
41
42
43
44
45
46
47
48
49

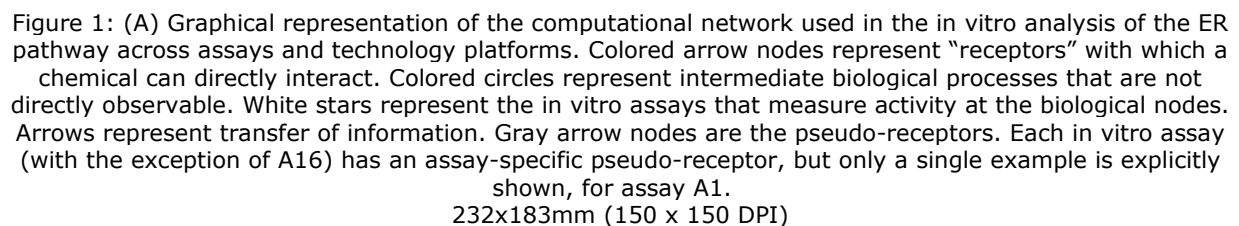
Table 3: The most potent 72 agonist and antagonist chemicals out of the 1812 tested. To be included in the list, either AUC(agonist) or AUC(antagonist) had to exceed 0.1, the median T had to be >50%, and the median Z had to be greater than 3. AUC values <0.001 are set to zero. Chemicals are ordered by decreasing value of AUC(R1).

CASRN	Name	Example Use	Structure Category	AUC (Agonist)	AUC (Antagonist)	Median AC50 (μM)	Median T	Median Z
57-91-0	17alpha-Estradiol	Pharmaceutical	steroid E	1.06	0	0.003	110	12.8
57-63-6	17alpha-Ethinylestradiol	Pharmaceutical	steroid E	1	0	0.001	100	14.4
84-16-2	meso-Hexestrol	Pharmaceutical	phenol-phenol [CC]	0.99	0	0.004	103	14.4
56-53-1	Diethylstilbestrol	Pharmaceutical	phenol-phenol [CC]	0.94	0.01	0.001	100	14.7
50-28-2	17beta-Estradiol	Pharmaceutical	steroid E	0.94	0.02	0.002	100	12.2
474-86-2	Equilin	Pharmaceutical	steroid E	0.82	0	0.01	118	18.9
53-16-7	Estrone	Pharmaceutical	steroid E	0.81	0.002	0.004	105	13.8
50-27-1	Estriol	Pharmaceutical	steroid E	0.79	0.01	0.03	108	17.0
72-33-3	Mestranol	Pharmaceutical	steroid E	0.74	0	0.07	107	15.9
17924-92-4	Zearalenone	Mycotoxin	carboxylic acid ketone	0.71	0	0.15	98	14.0
2971-36-0	HPTE	Pesticide degradate	phenol-phenol [C] halide	0.57	0.04	0.10	100	8.3
1478-61-1	Bisphenol AF	Plastics	phenol-phenol [C] halide	0.55	0	0.10	107	9.1
446-72-0	Genistein	Natural product	genistein-like	0.54	0	0.34	103	4.7
77-40-7	Bisphenol B	Plastics	phenol-phenol [C]	0.49	0.002	0.21	101	7.8
80-05-7	Bisphenol A	Plastics	phenol-phenol [C]	0.45	0	0.67	110	5.6
486-66-8	Daidzein	Flavone	genistein-like	0.44	0	1.3	107	4.5
84852-15-3	4-Nonylphenol, branched	Detergent ingredient	phenol alkyl	0.44	0	1.6	94	3.9
105624-86-0	5HPP-33	Pharmaceutical	thalidomide-like	0.42	0	0.98	89	4.8
104-43-8	4-Dodecylphenol	Industrial intermediate	phenol alkyl	0.41	0	1.1	84	4.6
521-18-6	5alpha-Dihydrotestosterone	Pharmaceutical	steroid A	0.4	0	2.8	86	3.5
131-55-5	2,2',4,4'-Tetrahydroxybenzophenone	UV-absorber	phenol-phenol [CO]	0.40	0	1.8	104	4.2

797-63-7	Norgestrel	Pharmaceutical	steroid P	0.39	0	0.44	95	7.5
140-66-9	4-(1,1,3,3-Tetramethylbutyl)phenol	Chemical intermediate	phenol alkyl	0.39	0	2.5	94	3.7
27193-86-8	Dodecylphenol	Chemical reactant/solvent	phenol alkyl	0.39	0	1.5	88	4.6
57-85-2	Testosterone propionate	Pharmaceutical	steroid A	0.39	0	3.4	100	3.7
789-02-6	o,p'-DDT	Insecticide	phenyl-phenyl [C] chloro	0.39	0	2.4	89	4.0
58-72-0	Triphenylethylene	Chemical reactant	triphenyl [C]	0.38	0	1.6	95	10.6
599-64-4	4-Cumylphenol	Industrial intermediate	phenol-phenyl [C]	0.38	0	2.3	99	4.1
5153-25-3	2-Ethylhexylparaben	Microbicide	paraben	0.37	0	2.3	102	4.0
53-43-0	Dehydroepiandrosterone	Pharmaceutical	steroid A	0.37	0	2.4	104	10.0
491-80-5	Biochanin A	Flavone	genistein-like	0.36	0	4.0	98	8.7
68-96-2	17alpha-Hydroxyprogesterone	Pharmaceutical	steroid P	0.34	0	0.36	105	13.0
27955-94-8	4,4',4-Ethane-1,1,1-triyltriphenol	Plastics	triphenol [C]	0.32	0	3.0	103	3.2
520-36-5	Apigenin	Flavone	genistein-like	0.31	0	2.1	95	9.8
80-46-6	4-(2-Methylbutan-2-yl)phenol	Chemical reactant	phenol alkyl	0.28	0	6.2	112	4.9
17696-62-7	Phenylparaben	Microbicide	paraben	0.28	0	5.7	122	7.4
1219-38-1	Octylparaben	Microbicide	paraben	0.27	0	5.7	81	3.2
131-56-6	2,4-Dihydroxybenzophenone	UV-absorber	phenol-phenyl [CO]	0.27	0	7.4	111	8.
80-09-1	4,4'-Sulfonyldiphenol	Chemical reactant	phenol-phenol [SO2]	0.26	0	22.5	98	6.3
520-18-3	Kaempferol	Flavone	genistein-like	0.25	0	4.0	76	9.0
6088-51-3	6-Hydroxy-2-naphthyl disulfide	Unknown	phenolnaphthalene-phenolnaphthalene [SS] alcohol	0.25	0	5.4	84	3.7
5349-51-9	4-(2-Methylbutan-2-yl)cyclohexanol	Fragrance agent	alcohol sec alkane cyclo	0.25	0	16.2	90	3.5
53-19-0	o,p'-DDD	Pesticide degradate	phenyl-phenyl [C] chloro	0.24	0	7.4	66	3.1
92-69-3	4-Phenylphenol	Chemical reactant	phenol-phenylphenol-2	0.22	0	13.9	124	7.1
94-13-3	Propylparaben	Microbicide	paraben	0.21	0	20.6	136	6.4
63-05-8	4-Androstene-3,17-dione	Pharmaceutical	steroid A	0.18	0	0.03	86	10.4
126-00-1	Diphenolic acid	Plasticizer	phenol-phenol [C] carboxylic acid	0.17	0	41.9	100	5.2

99-71-8	4-(Butan-2-yl)phenol	Chemical intermediate	phenol alkyl	0.16	0	20.4	101	6.4
98-54-4	4-tert-Butylphenol	Plasticizer	phenol alkyl	0.16	0	21.5	89	6.3
14816-18-3	Phoxim	Insecticide	phenyl thiophosphate nitrile	0.16	0	25.8	64	6.0
2919-66-6	Melengestrol acetate	Pharmaceutical	steroid P	0.16	0	0.03	97	17.4
124-22-1	1-Dodecanamine	Surfactant	amine pri	0.15	0	5.4	70	4.8
6683-19-8	Irganox 1010	Antioxidant	phenol carboxylate chelator 4	0.15	0	14.2	83	7.0
51-52-5	6-Propyl-2-thiouracil	Pharmaceutical	uracil	0.14	0	7.7	66	8.0
612-82-8	3,3'-Dimethylbenzidine dihydrochloride	Chemical reactant (dyes)	aniline-aniline	0.14	0	0.04	89	8.1
4712-55-4	Diphenyl phosphite	Stabilizer (PVC)	phenyl phosphate	0.14	0	34.8	64	5.5
141-79-7	4-Methylpent-3-en-2-one	Solvent	ketone ene	0.14	0	17.2	83	6.70
2/3/6893	3,5,3'-Triiodothyronine	Pharmaceutical	phenol-phenyl [O] iodo carboxylic acid	0.14	0	10.4	69	7.53
6055-19-2	Cyclophosphamide monohydrate	Pharmaceutical	phosphamide	0.14	0	13.2	74	7.1
480-40-0	Chrysin	Flavone	phenol benzopyran	0.13	0	10.7	79	7.3
3319-31-1	Tris(2-ethylhexyl) trimellitate	Plastics	phthalate	0.12	0	44.6	76	5.1
1638-22-8	4-Butylphenol	unknown	phenol alkyl	0.11	0	17.4	91	6.7
140-10-3	Cinnamic acid	Flavor agent/Fragrance agent	phenyl carboxylic acid	0.10	0	25.8	68	5.8
960-71-4	Triphenylborane	Chemical intermediate	triphenyl [B]	0.10	0	47.0	71	5.0
50-41-9	Clomiphene citrate	Pharmaceutical	tamoxifen-like	0.03	0.59	0.04	124	8.3
54965-24-1	Tamoxifen citrate	Pharmaceutical	tamoxifen-like	0.03	0.55	0.16	136	6.5
82640-04-8	Raloxifene hydrochloride	Pharmaceutical	phenol-phenol	0.02	0.67	0.01	131	12.3
10540-29-1	Tamoxifen	Pharmaceutical	tamoxifen-like	0.02	0.45	0.28	131	6.1
68392-35-8	4-Hydroxytamoxifen	Pharmaceutical	tamoxifen-like	0.01	0.69	0.04	115	10.6
90357-06-5	Bicalutamide	Pharmaceutical	flutamide-like	0.003	0.11	9.7	57	7.3
84371-65-3	Mifepristone	Pharmaceutical	steroid P	0.003	0.31	2.0	110	4.1
129453-61-8	Fulvestrant	Pharmaceutical	steroid E	0	0.64	0.04	113	7.1

1
2
3
4
5
6
7
8
9
10
11
12
13
14
15
16
17
18
19
20
21
22
23
24
25
26
27
28
29
30
31
32
33
34
35
36
37
38
39
40
41
42
43
44
45
46
47
48
49



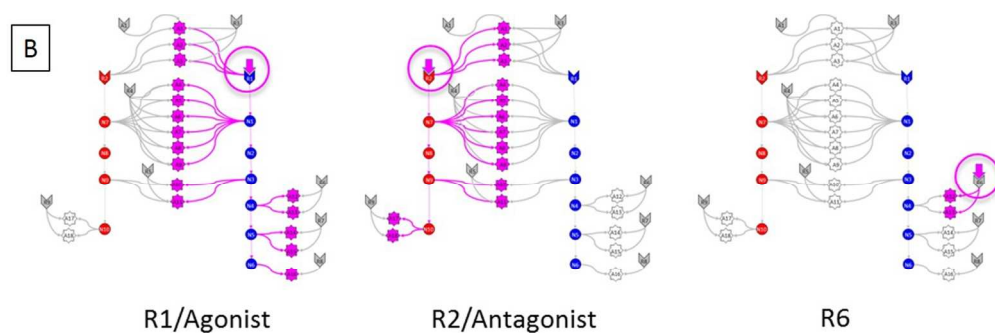


Figure 1: (B) Patterns of assays that would be activated when specific receptors are activated by the chemical, in particular R1, R2 and R6. The activating chemical in its receptor are circled in pink, and the activated assays and the pathways to them are also highlighted in pink.
229x77mm (150 x 150 DPI)

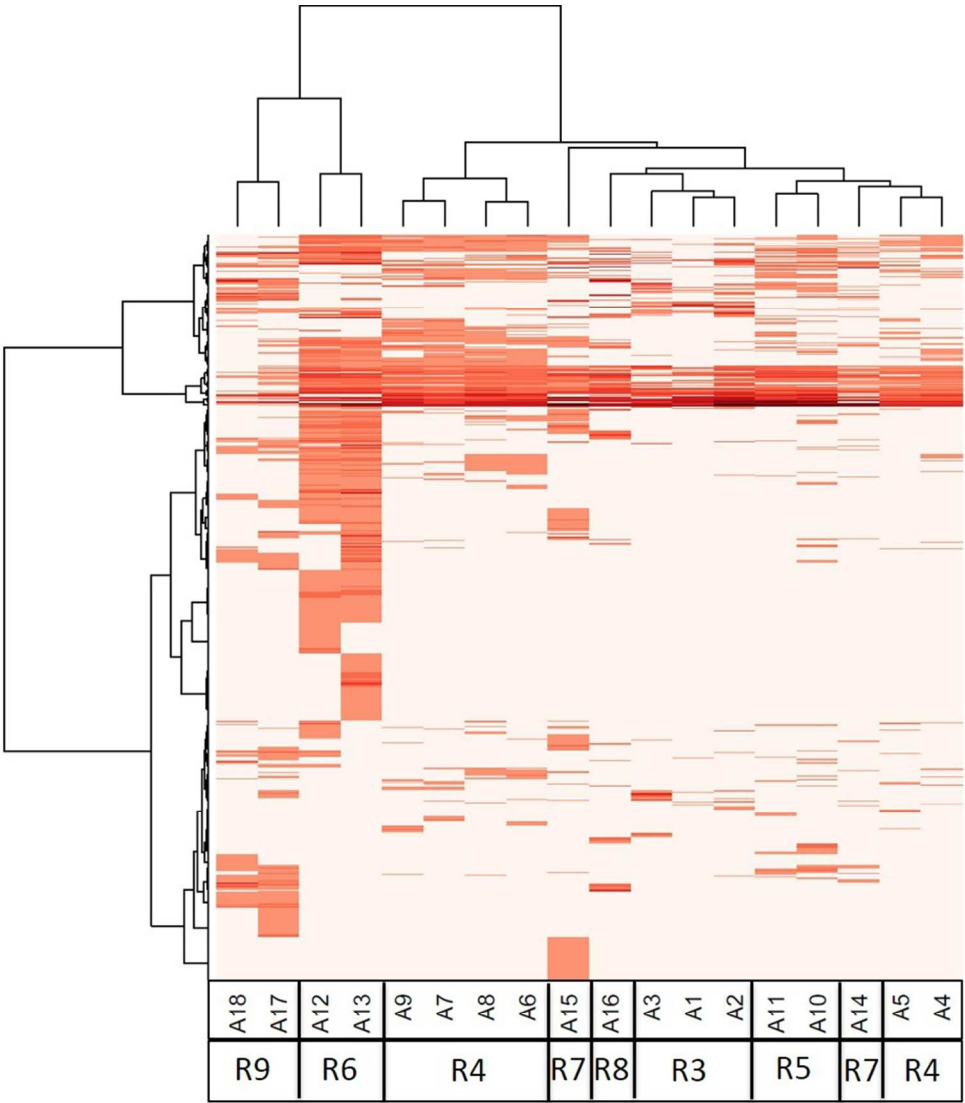


Figure 2: Two-way hierarchical clustering of chemical activity across the 18 in vitro assays used to test for ER activity. The heatmap shows $-\log_{10}(\text{AC}_{50})$ values for all assays and all chemicals with at least one assay hit. Darker red indicates more potent activity (lower AC_{50}), while white represents inactive chemical-assay pairs. Note that the assays cluster by technology / pseudo-receptor. The "A" and "R" values refer to the assay and receptors/pseudo-receptors from Figure 1 and Table 1.

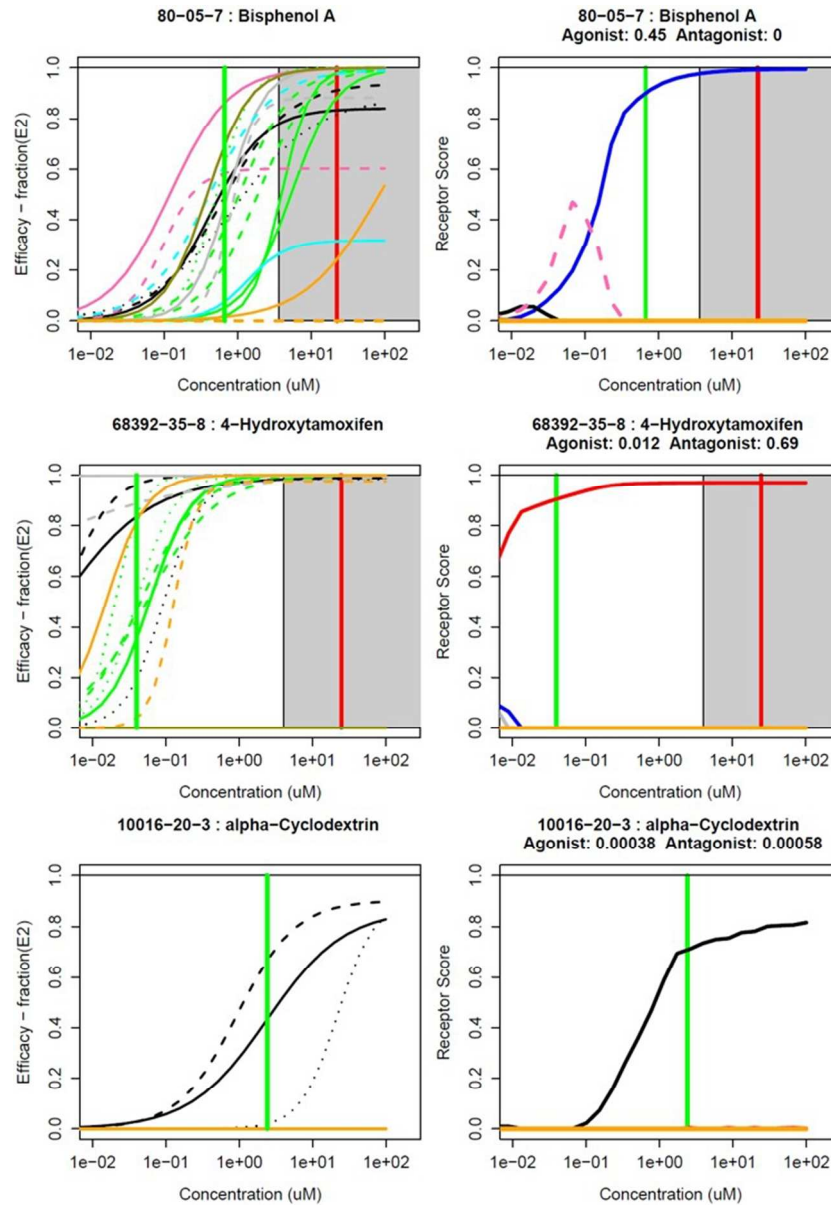


Figure 3: Results of the model for three prototype chemicals. For each chemical, the left-hand panel shows the synthetic concentration-response data for the 18 assays, colored by assay group defined the legend. The right-hand panel shows the corresponding magnitude of the modeled receptor responses. The agonist receptor (R1) is designated by blue, the antagonist receptor (R2) by red and the other pseudo-receptors are colored as indicated in the legend. AUC values for the agonist (R1) and antagonist (R2) receptors are provided below the chemical name. For chemicals with the cytotoxicity burst defined (2 or more cytotoxicity hits, see Methods), the burst center is indicated by a vertical red line, and the burst region (starting 3 burst MAD below the burst center) is indicated by the gray shaded region. A green horizontal bar indicates the median-AC50 of the active assays. Similar plots for all chemicals are given in Supplemental File S3.

127x182mm (150 x 150 DPI)

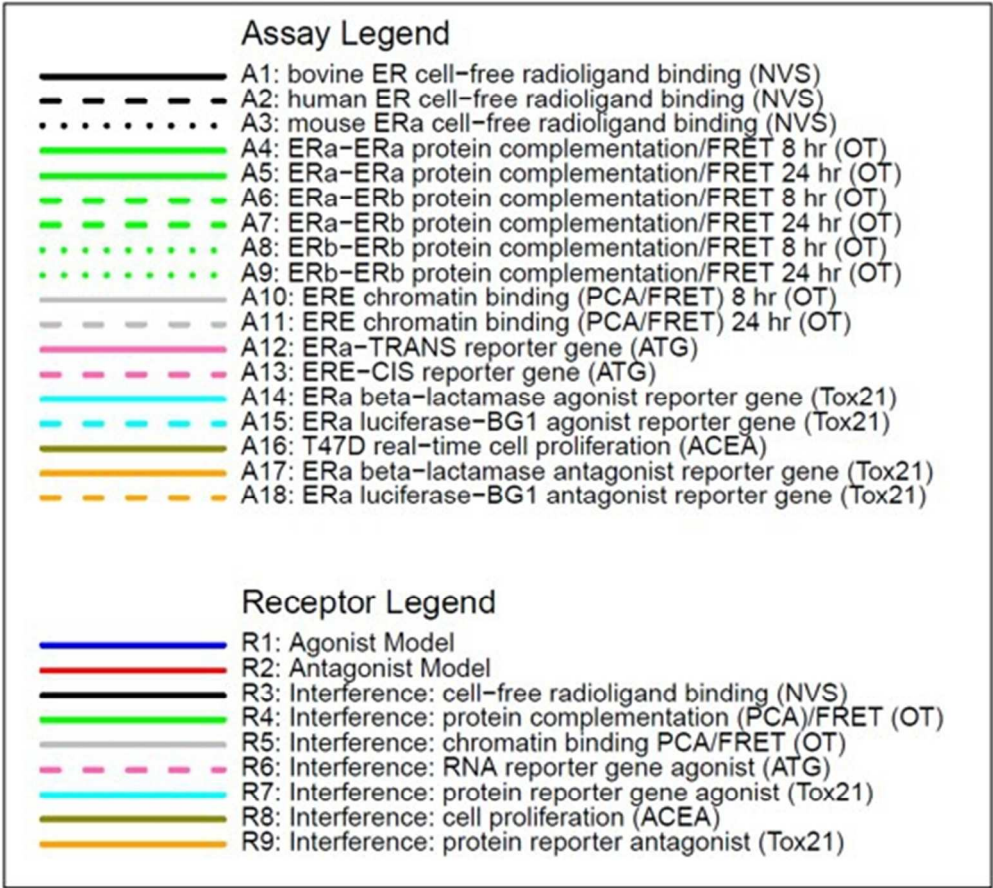


Figure 3 legend
91x82mm (150 x 150 DPI)

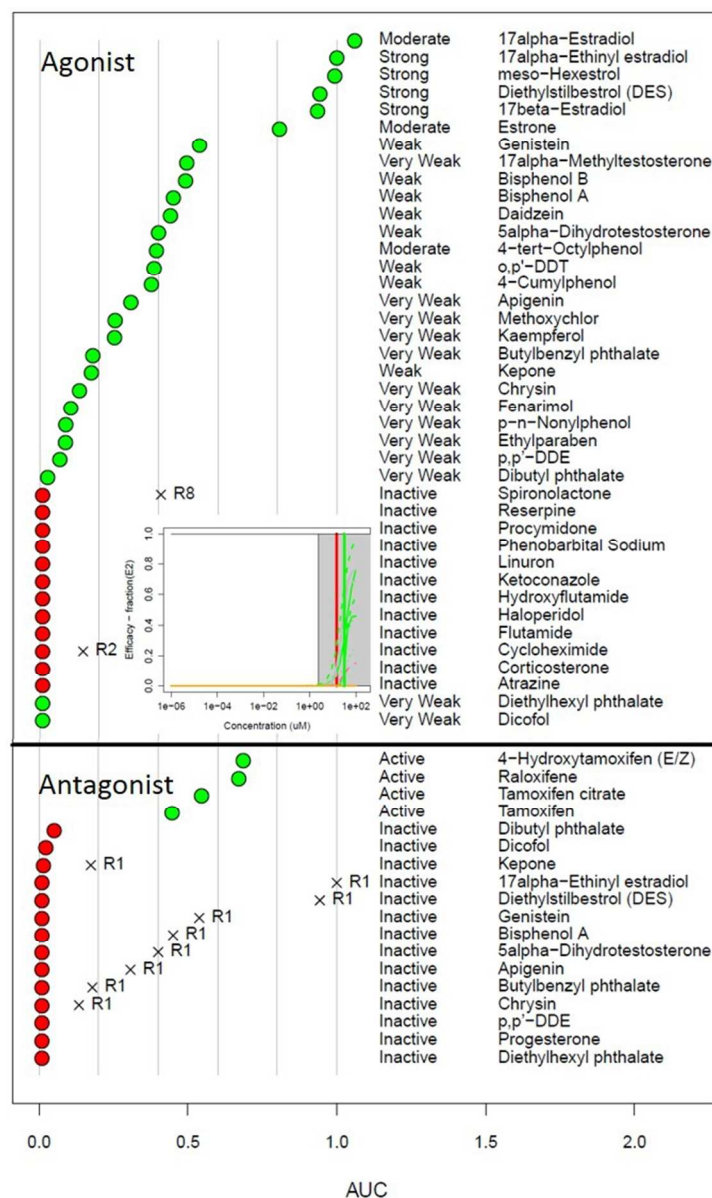


Figure 4: Plots showing activity of the agonist (top) and antagonist (bottom) reference chemicals. Chemicals that are intended to be positive are indicated by green circles, while those intended to be inactive are indicated by red circles. For the agonists, the expected potency range is also indicated (middle column). For chemicals with one or more pseudo-receptor AUC values greater than zero, the value is indicated by an X, and the pseudo-receptor name is indicated. The inset shows the assay curves for dibutyl phthalate, as described in the text (colored based on Figure 3).

114x191mm (150 x 150 DPI)

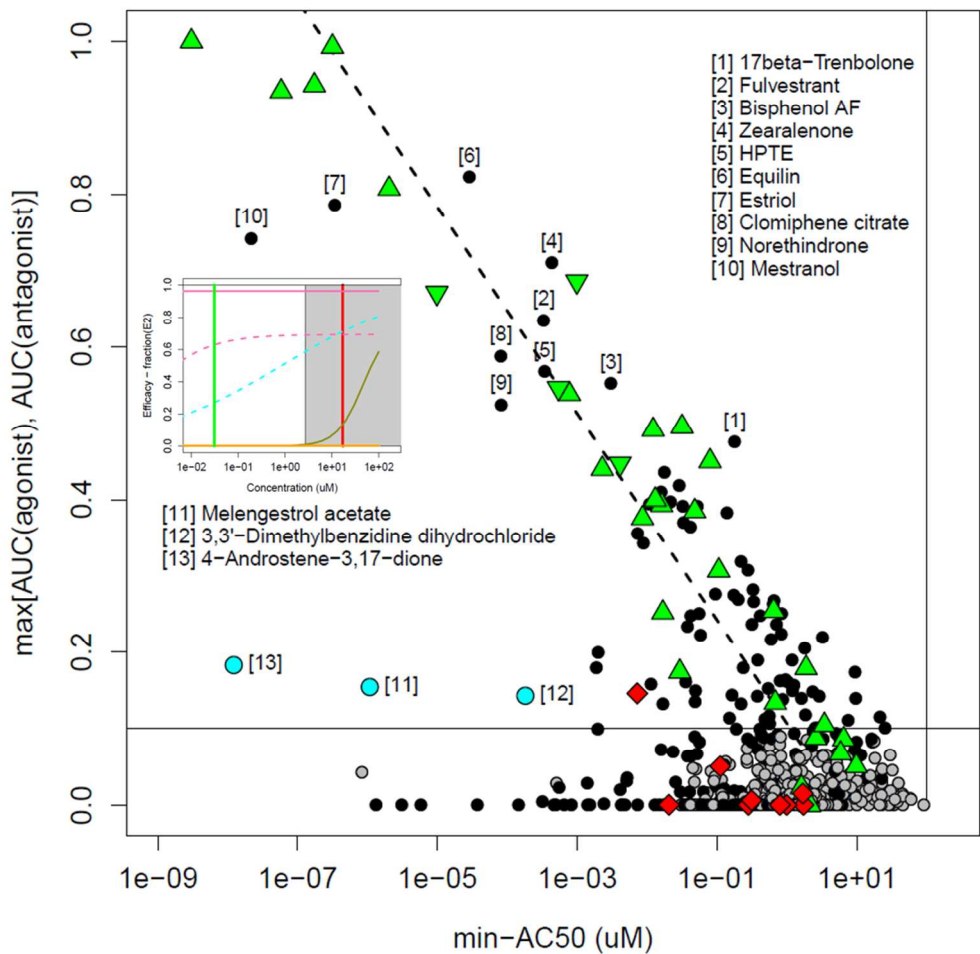


Figure 5: Plot of the maximum AUC vs. minimum-AC50 values. Each point is a single chemical that was active in at least one assay. The AUC value given is the maximum of the AUC(agonist) and AUC(antagonist) values for the chemical. The dashed line is the best-fit for AUC(agonist) values > 0.1. Chemicals are labeled in order: black circle, at least one AUC > 0.1; green up-arrow, positive agonist reference chemical; green down-arrow, positive antagonist reference chemical; red diamond, negative reference chemical; cyan circle, example chemicals with AUC significantly below the fitted line but above 0.1. The vertical line at 100 μ M indicates the highest concentration tested, while the horizontal line at AUC = 0.1 indicates an approximate threshold between chemicals with clear agonist / antagonist activity and those that are potentially active through interference processes. The inset shows graphs of assay activity for 4-androstene-3,17-dione (colored based on Figure 3).
192x185mm (150 x 150 DPI)

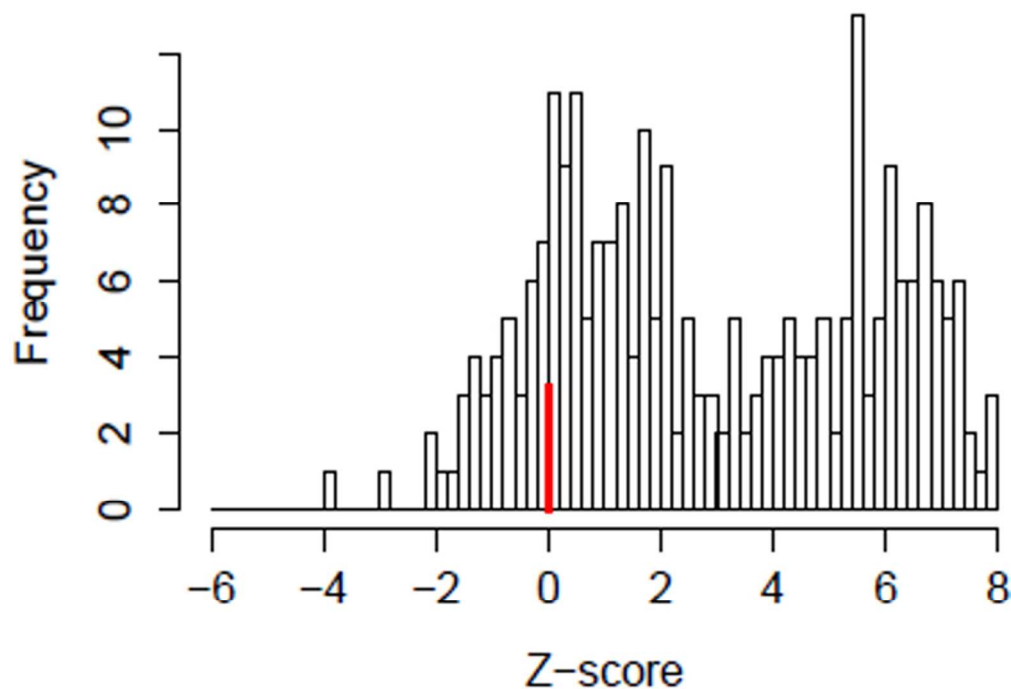


Figure 6: Histogram of Z-scores for the assay ATG_ERa_TRANS_up. The Z-score is defined as the distance between the median cytotoxicity concentration and a chemical's AC50 in this assay, in units of global cytotoxicity MAD, for all chemicals active in this assay. One can see a bimodal distribution with one peak at zero (marked with a heavy red line) and another with a peak near 6. We hypothesize that chemicals active in the low-Z region are more likely to be false positives and less likely to be estrogenic than those active in the high-Z region.

131x91mm (150 x 150 DPI)

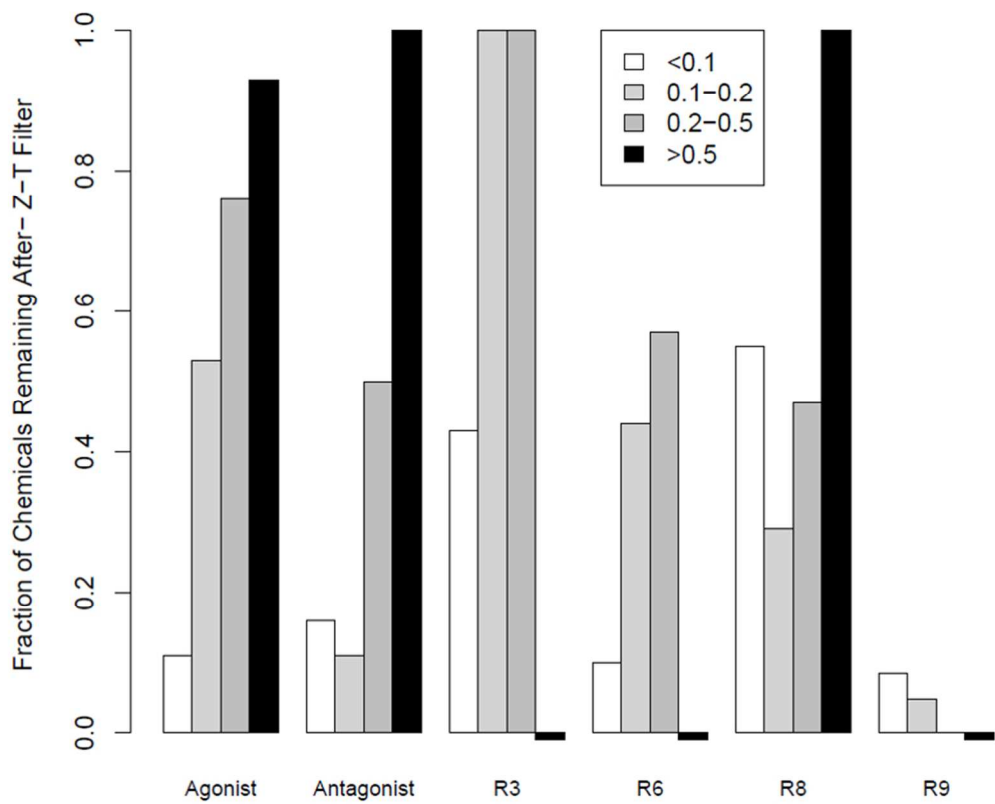


Figure 7: Bar chart showing the fraction of chemicals remaining for each of the multi-assay receptors / pseudo-receptors after filtering for efficacy (T) and cytotoxicity (Z-score). The receptors were limited to those with 5 or more chemicals with AUC>0.1 from Table 2. If there were no chemicals for a pseudo-receptor in a given AUC bin, a small negative bar is shown. The legend indicates AUC ranges corresponding to Table 2.

207x169mm (105 x 105 DPI)